Cancer Therapy: Preclinical

Clinical Cancer Research

Amiloride, An Old Diuretic Drug, Is a Potential Therapeutic Agent for Multiple Myeloma

Elizabeta A. Rojas[1,2], Luis Antonio Corchete[1,2,3], Laura San-Segundo[1,2], Juan F. Martínez-Blanch[4], Francisco M. Codoñer[4], Teresa Paíno[1,2], Noemí Puig[1,2,3], Ramón García-Sanz[1,2,3], María Victoria Mateos[1,2,3], Enrique M. Ocio[1,2,3], Irena Misiewicz-Krzeminska[1,2,5], and Norma C. Gutiérrez[1,2,3]

Abstract

Purpose: The search for new drugs that control the continuous relapses of multiple myeloma is still required. Here, we report for the first time the potent antimyeloma activity of amiloride, an old potassium-sparing diuretic approved for the treatment of hypertension and edema due to heart failure.

Experimental Design: Myeloma cell lines and primary samples were used to evaluate cytotoxicity of amiloride. *In vivo* studies were carried out in a xenograft mouse model. The mechanisms of action were investigated using RNA-Seq experiments, qRT-PCR, immunoblotting, and immunofluorescence assays.

Results: Amiloride-induced apoptosis was observed in a broad panel of multiple myeloma cell lines and in a xenograft mouse model. Moreover, amiloride also had a synergistic effect when combined with dexamethasone, melphalan, lenalidomide, and pomalidomide. RNA-Seq experiments showed that amiloride not only significantly altered the level of transcript isoforms and alternative splicing events, but also deregulated the spliceosomal machinery. In addition, disruption of the splicing machinery in immunofluorescence studies was associated with the inhibition of myeloma cell viability after amiloride exposure. Although amiloride was able to induce apoptosis in myeloma cells lacking p53 expression, activation of p53 signaling was observed in wild-type and mutated *TP53* cells after amiloride exposure. On the other hand, we did not find a significant systemic toxicity in mice treated with amiloride.

Conclusions: Overall, our results demonstrate the antimyeloma activity of amiloride and provide a mechanistic rationale for its use as an alternative treatment option for relapsed multiple myeloma patients, especially those with 17p deletion or *TP53* mutations that are resistant to current therapies. *Clin Cancer Res; 23(21); 6602–15. ©2017 AACR.*

Introduction

Despite improvements in the survival of multiple myeloma patients thanks to the introduction of novel therapeutic agents (1, 2), it remains an incurable disease (3). Multiple myeloma initially responds to chemotherapy but relapse and chemoresistance usually occur (4), so subsequent recurrences are part of its natural history. Therefore, the search for new drugs that control the disease continues to be required.

Great efforts to develop new agents against multiple myeloma have been made in recent years, to the extent that a wide array of new agents with different mechanisms of action have recently been approved. These include new mAbs, proteasome inhibitors, immunomodulatory drugs and histone deacetylase inhibitors, among others (5). However, their approval processes required several years of research and major investment. An interesting alternative by which this long process might be shortened is the drug-repositioning approach, which involves using old drugs approved for noncancerous diseases (6). One of the advantages of this strategy is that the pharmacokinetic and pharmacodynamic properties and toxicity profiles tend to be well known. The diuretic drug, amiloride, is one such agent.

Amiloride is a potassium-sparing diuretic that has been employed clinically for more than three decades in the treatment of hypokalemia, hypertension, edema and congestive heart failure (7). Some studies demonstrated its significant antitumor and antimetastasis activities that were initially associated with the inhibition of Na^+/H^+ exchangers (8). Recently, amiloride was found to modify alternative splicing (AS) in various human cancer cells (9). Pre-mRNA alternative splicing is a highly regulated process, and numerous studies have demonstrated its aberrations to be associated with cancer, tumor progression, and metastasis. This mechanism has recently gained attention as a potential therapeutic target for cancer due to the differential splicing patterns identified in tumor cells and metastatic tumor populations (10–14).

In this study, we evaluated for the first time the antimyeloma (anti-multiple myeloma) effect of amiloride using *in vitro, ex vivo,* and *in vivo* models. We found that amiloride had potent activity against a broad panel of multiple myeloma cell lines regardless of

[1]Cancer Research Center-IBMCC (USAL-CSIC), Salamanca, Spain. [2]Institute of Biomedical Research of Salamanca (IBSAL), Salamanca, Spain. [3]Hematology Department, University Hospital of Salamanca, Spain. [4]Lifesequencing S.L., Valencia, Spain. [5]National Medicines Institute, Warsaw, Poland.

Note: Supplementary data for this article are available at Clinical Cancer Research Online (http://clincancerres.aacrjournals.org/).

I. Misiewicz-Krzeminska and N.C. Gutiérrez contributed equally to this article.

Corresponding Author: Norma C. Gutiérrez, Department of Hematology, University Hospital of Salamanca, Paseo San Vicente, 58-182, Salamanca 37007, Spain. Phone: 349-2329-1384; Fax: 349-2329-4624; E-mail: normagu@usal.es

doi: 10.1158/1078-0432.CCR-17-0678

Translational Relevance

The investigation of novel therapeutic agents is needed to manage the multiple relapses arising from resistant clones in multiple myeloma. In this study, we demonstrate for the first time the antimyeloma activity of amiloride, a very well-known drug used in the treatment of hypokalemia, hypertension, and edema. This finding together with the manageable toxicity profile of amiloride provide the rationale for conducting clinical trials that support the repositioning of this old drug for the treatment of multiple myeloma. Moreover, our results showed that multiple myeloma cells either with WT or mutated *TP53* were highly sensitive to amiloride, which makes this drug an attractive candidate for high-risk myeloma patients with *TP53* abnormalities.

TP53 status. In addition, RNA-Seq experiments showed a strong alteration of spliceosome functionality. These encouraging findings, in conjunction with the manageable toxicity profiles of amiloride, provide a framework for evaluating its utility in clinical trials.

Materials and Methods

Reagents and multiple myeloma cells

The human myeloma cell lines, NCI-H929, MM1S, MM1R, and U266 were acquired from ATCC, RPMI-8226, KMS12-BM, KMS12-PE, and JJN3 from DMSZ (Deutsche Sammlung von Mikroorganismen and Zellkulturen). RPMI-LR5 cell line was kindly provided by Dr. W.S. Dalton (Moffitt Cancer Center, Tampa, FL). All cell lines were cultured in RPMI1640 medium supplemented with 10% FBS and antibiotics (Gibco). Cells were routinely checked for the presence of mycoplasma with MycoAlert kit (Lonza). Cell line identity was confirmed periodically by STR analysis with PowerPlex 16 HS System kit (Promega) and online STR matching analysis (www.dsmz.de/fp/cgi-bin/str.html). All multiple myeloma samples from patients and cells from healthy donors were cultured in AIMV medium supplemented with 20% FBS (Thermo Fisher Scientific). $CD138^+$ plasma cells from bone marrow samples of 8 patients with multiple myeloma were isolated using an autoMACS separation system (Miltenyi-Biotec). Clinical information of the patients included in the study is summarized in Supplementary Materials.

Amiloride and melphalan were purchased from Sigma-Aldrich, bortezomib was from LC Laboratories, dexamethasone was from Merck KGaA, and lenalidomide and pomalidomide from Selleckchem. All multiple myeloma patients as well as healthy donors involved in the study provided written informed consent in accordance with the Helsinki Declaration. The research ethics committee of the University Hospital of Salamanca approved the study.

Cell viability assays

Cell viability and proliferation were evaluated using CellTiter-Glo (Promega) and 3 (4,5-dimethylthiazol-2-yl)-2,5-diphenyltetrazolium bromide (MTT) colorimetric assay (Sigma-Aldrich), respectively, as described previously (15, 16). Synergism between amiloride and other drugs was evaluated with CalcuSyn software (Biosoft; ref. 17; Supplementary Material).

Apoptosis and cell-cycle assays

Apoptosis using Annexin V-FITC/propidium iodide (PI) double staining, mitochondrial membrane depolarization using DilC1(5) (Immunostep) and cell-cycle analysis, were performed by flow cytometry using Infinicyt software (Cytognos S.L.), as described previously (15). Caspases-3/7, 8, and 9 activities were evaluated by Caspase Glo 3/7, Caspase-Glo 8, and Caspase-Glo 9 assays (Promega), respectively, according to the manufacturer's protocol.

Ex vivo analysis of cytotoxicity in freshly total bone marrow cells

The experiments with patient's cells were performed in total bone marrow samples from patients with multiple myeloma. Immediately after extraction, total bone marrow samples were lysed with ammonium chloride to remove red blood cells (erythrocytes); the remaining white blood cells were maintained for 48 hours in AIMV medium supplemented with 20% FBS (Thermo Fisher Scientific) in the absence or presence of different concentrations of amiloride. Then, the activity of amiloride was investigated on plasma cells (PC) and on the main bone marrow cell populations separately. To evaluate the cytotoxicity of amiloride on PCs, samples were analyzed using Annexin V (Immunostep) in combination with three markers that allowed for the identification of pathologic PCs present in the sample. With that aim, we used a fix combination of two mAbs (CD38 and CD45) plus a third one, chosen depending on the specific phenotype of each patient's clonal plasma cells (usually CD56 or CD19). The cells were incubated for 15 minutes at room temperature in the dark. A total of 5×10^5 cells were acquired on a FACSCanto II flow cytometer (BD Biosciences). Finally, apoptosis was analyzed in pathologic PCs (gated on $CD38^{++}$ and $CD56^{+/-}$, or $CD19^{+/-}$ and FSC/SSC) using the Infinicyt software. Annexin V–positive events among the target populations were considered apoptotic cells.

Amiloride cytotoxicity on the other bone marrow cell populations, that is B and T lymphocytes, NK cells and granulocytes, was assessed with the same aforementioned protocol described, but including a panel of 5 antibodies in combination with Annexin V to identify T lymphocytes ($CD3^+$), B lymphocytes ($CD19^+$), NK cells ($CD56^+/CD3^-$), and granulocytes ($SSC^{high}/CD45+^{dim}$). Among each of these populations separately, we identified as apoptotic the percentage being Annexin V positive using the Infinicyt software.

Multiple myeloma xenograft murine model

All animal experiments were performed according to the institutional guidelines and the protocol previously approved by the ethical committee of the University of Salamanca (Salamanca, Spain). For the human subcutaneous plasmacytoma model, 65 CB17-SCID mice (The Jackson Laboratory) were subcutaneously inoculated into the right flank with 3×10^6 MM1S cells in 100 μL of RPMI1640 medium and 100 μL of Matrigel (BD Biosciences). Treatment was initiated immediately after tumor cell inoculation and mice were randomized to the following treatment cohorts, each of five animals: vehicle-alone PBS (C); amiloride, 10 mg/kg (A10); amiloride, 15 mg/kg (A15); dexamethasone, 0.5 mg/kg (D); melphalan, 2.5 mg/kg (M), dexamethasone + melphalan (DM); dexamethasone + amiloride, 10 mg/kg (DA10); melphalan + amiloride, 10 mg/kg (MA10); dexamethasone + melphalan + amiloride, 10 mg/kg (DMA10); dexamethasone + amiloride, 15 mg/kg (DA15); melphalan + amiloride, 15 mg/kg (MA15);

and dexamethasone + melphalan + amiloride, 15 mg/kg (DMA15). Amiloride was administered orally daily, and dexamethasone and melphalan intraperitoneally (i.p.) two days a week. Tumor burden estimation and toxicity monitoring were performed as described previously (18).

To estimate survival, mice were sacrificed when the diameter of their tumor reached 2 cm or when they became moribund. Time to endpoint (TTE) was estimated from the day of treatment initiation. For *in vivo* mechanistic studies, six and four mice, respectively, were subcutaneously inoculated in the right flank with 3×10^6 MM1S cells and 3×10^6 RPMI cells. When the tumor attained a large volume, mice were randomized to receive the vehicle-alone PBS (control group) or amiloride (20 mg/kg) orally for two consecutive days. On the third day, mice were sacrificed and the tumors retrieved for analysis.

RNA sequencing

Poly A^+ RNA from KMS12-BM and JJN3 cells untreated or treated with amiloride (0.1 mmol/L and 0.4 mmol/L, respectively) for 24 hours was isolated and prepared for RNA sequencing (RNA-Seq). Libraries were constructed following a TruSeq Stranded mRNA Sample Preparation Guide (Illumina). The final cDNA library was sequenced using Illumina HiSeq 2500 in combination of 100 Paired-End at Lifesequencing S.L. (Supplementary Material).

RNA-Seq analysis

Paired-end FASTQ files for 12 samples were used in the RNA-Seq analyses. We analyzed the data in three stages: gene expression, isoform level, and splicing events. First, in the analysis of differential expression at the gene level, the genes were considered to be differentially expressed for an absolute n-fold change (FC) of $\geq$2 and a false discovery rate (FDR) of <0.05. Second, in the analysis of isoform level, we focused on the isoforms with an absolute value of FC $\geq$ 2 and that corresponded to genes without altered total expression. The criteria used to assign genes as "no-change" were FDR > 0.05 and an absolute value of FC < 2, when the DESeq2 package was applied. Third, differential alternative splicing events were detected using rMATS version 3.0.9 (19), classifying these events into five major types of pattern: skipped exon (SE), alternative 5′ splice site (A5SS), alternative 3′ splice site (A3SS), mutually exclusive exons (MXE), and retained introns (RI). rMATS also calculates the difference in the ratio of these events between two conditions, and produces an estimate of the FDR. Finally, all the enrichment analyses were conducted using the Webgestalt web tool (20), employing the Gene Ontology and KEGG databases as data sources. The dataset is available at the Gene Expression Omnibus (GEO) repository (http://www.ncbi.nlm.nih.gov/geo) under the accession number GSE95077.

Further details are provided in the Supplementary Material.

RNA extraction and quantitative real-time PCR analysis

RNA was extracted using the RNeasy Plus Mini kit (Qiagen). The RNA integrity was assessed with an Agilent 2100 Bioanalyzer (Agilent Technologies). Total RNA (1 μg) was reverse-transcribed to cDNA using High-Capacity cDNA Reverse Transcription Kit (Applied Biosystems). Gene expression was quantified by TaqMan qRT-PCR mRNA assays (Applied Biosystems) and normalized relative to 18S5 using the $2^{-\Delta C_t}$ method.

Immunoblotting and immunofluorescence analysis

Western blot methods and the preparation of protein lysates have been described elsewhere (15). The sources of the mAbs are described in the Supplementary Material.

For immunofluorescence, cells were fixed in 4% paraformaldehyde, permeabilized with 0.25% Triton X-100/PBS, stained with primary mouse anti-SC35 (Abcam) and goat anti-mouse IgG (H+L) secondary antibody, and Alexa Fluor 488 conjugate (Thermo Fisher Scientific). Fluorescence was measured under a Leica confocal microscope.

Statistical analysis

All statistical analyses were carried out with IBM SPSS Statistics 22.0 (IBM Corp.) and the Simfit package (W.G. Bardsley, University of Manchester, Manchester, UK; v7.0.9 Academic 32-bit, http://www.simfit.org.uk/). *P* values were corrected for multiple testing using the FDR, with values of <0.05 being considered to be statistically significant. Differences in the *in vitro* experiments are expressed as the mean ± SD of at least three determinations and were assessed by the two-sided Student *t* test or the Mann–Whitney *U* test. Differences in tumor volumes between groups were evaluated fitting an exponential regression model and the regression parameters were compared using a *t* test for unequal variances. Survival curves were plotted using the Kaplan–Meier method, and compared using the log-rank test.

Results

Amiloride is cytotoxic for multiple myeloma and potentiates the efficacy of various antimyeloma agents

Amiloride exhibited potent *in vitro* antimultiple myeloma activity in a dose- and time-dependent manner, as demonstrated in a panel of seven myeloma cell lines with a wide range of cytogenetic abnormalities and p53 status (Supplementary Table S1; Supplementary Fig. S1A). The viability was significantly reduced in both the *TP53* wild-type (WT; H929, MM1S) and the mutated *TP53* cell lines (KMS12-BM, KMS12-PE, U-266, and RPMI-8226) after exposure to amiloride ($P < 0.01$; Fig. 1A), although viability reduction in the p53-null cell line JJN3 required a higher dose and a longer time course ($P < 0.01$). The antimultiple myeloma effect of amiloride was also observed in melphalan- and dexamethasone-resistant cell lines, RPMI-LR5 and MM1R, respectively (Supplementary Fig. S2A).

In the *ex vivo* study using bone marrow cells from 10 patients with multiple myeloma (six newly diagnosed and four relapsed/refractory), we observed significant apoptosis induction in plasma cells, even in three patients bearing deletion of 17p, with minor cytotoxicity toward B and T lymphocytes, NK cells, and neutrophils (Fig. 1B). Myeloma cell cytotoxicity of amiloride was also confirmed on isolated $CD138^+$ plasma cells from eight multiple myeloma patients (Supplementary Fig. S1B). Interestingly, amiloride did not induced cytotoxicity on normal plasma cells from healthy donors (Supplementary Fig. S1C).

Next, we evaluated the cytotoxicity of double combinations of amiloride with melphalan and dexamethasone, employing a constant ratio between them. Subsequent isobologram analysis revealed a combination index (CI) in the synergistic range for the double combinations of amiloride with dexamethasone or melphalan, ranging from 0.2 to 0.8, depending on the doses

and cell lines used (Fig. 1C; Supplementary Fig. S2B). Furthermore, amiloride overcame the melphalan and dexamethasone resistance of RPMI-LR5 and MM1R, respectively (Supplementary Fig. S2C and S2D). Amiloride was also combined with new agents such as lenalidomide, pomalidomide and bortezomib. A significant synergism was observed between amiloride and lenalidomide or pomalidomide plus dexamethasone (Fig. 1D and E). In contrast, the combination of amiloride with bortezomib was antagonistic in all cell lines tested (Supplementary Fig. S2E).

To test whether amiloride was able to inhibit the protective effect of the bone marrow microenvironment, MM1S-luc cells were cocultured with mesenchymal stem cells (MSC) from six multiple myeloma patients and treated with increasing concentrations of amiloride for 48 hours. Despite the proliferative advantage to multiple myeloma cells conferred by MSCs, amiloride abrogated the protective effect conferring by MSCs. In contrast, MSCs were resistant to the cytotoxic effect of amiloride (Supplementary Fig. S3).

Amiloride induces apoptosis and enhances mitochondrial depolarization

To elucidate the mechanisms leading to the decrease of cell growth induced by amiloride, we analyzed cell cycle and apoptosis in multiple myeloma cell lines treated with increasing concentrations of the drug (0.1–1.0 mmol/L). Amiloride induced significant apoptosis after 24 and 48 hours in H929, KMS12-BM and JJN3 cell lines (Fig. 2A; Supplementary Fig. S4A), as well as in MM1S, U-266 and RPMI cell lines after 48 hours (Supplementary Fig. S4B). The apoptosis induction was dose-dependent in all cell lines, with the highest levels in the KMS12-BM cell line, even at 0.1 mmol/L after 24 hours of treatment (Fig. 2A). It is of particular note that the apoptosis induced by amiloride was also observed in cells with del(17p) or *TP53* mutations (JJN3 and KMS12-BM, respectively). No significant effect of amiloride on cell cycle was observed (Supplementary Fig. S5).

To evaluate the involvement of mitochondria in cell death, the membrane potential ($\Delta\psi_m$) was measured. Amiloride caused a decrease in $\Delta\psi_m$, particularly significantly in KMS12-BM, H929, and RPMI-8226 cells (Fig. 2B; Supplementary Fig. S6). Using a luminescent-proteolytic assay, we observed that the caspases 3/7, 8, and 9 were significantly activated in all the cell lines tested (Fig. 2C; Supplementary Fig. S7A). The involvement of a caspase-independent mechanism was also observed, as Z-VAD-FMK, a pan-caspase inhibitor, was able to inhibit caspase-3/7 activity, but unable to inhibit apoptosis induced by amiloride (Supplementary Fig. S7B).

***In vivo* antimyeloma efficacy of amiloride**

We evaluated the *in vivo* efficacy of amiloride (A) in monotherapy and in combination with melphalan (M) and dexamethasone (D). As to the best of our knowledge, there are no data concerning the antitumor efficacy of amiloride in the animal model used here, we evaluated two doses of amiloride (10 mg/kg and 15 mg/kg). Treatment of MM1S-inoculated CB17-SCID mice with a double or triple combination of A (regardless of the A dose applied), together with D and/or M, enhanced tumor growth inhibition, although the differences were only statistically significant for the combinations DA10, DA15, and DMA15 (Fig. 3A; Supplementary Fig. S8A). With respect to survival, we observed a significant improvement in TTE in the group of mice treated with the double combinations, DA10 and MA10, and the triple combination, DMA10, compared with the D, M, and DM groups, respectively ($P < 0.05$; Fig. 3B). The mice treated with the triple combination DMA10 had a median overall survival (OS) of 115 days compared with 99 days for the combination DM ($P < 0.05$; Fig. 3B). The double combinations, DA15 and MA15, also showed a statistically significant benefit ($P < 0.01$) in terms of OS compared with the single drugs (Supplementary Fig. S8B). The triple combination DMA15 also had a longer OS (median, 110 days) than the double combination DM (median, 99 days), although the difference was not statistically significant ($P = 0.053$; Supplementary Fig. S8B). No significant toxicity, measured as body weight loss, was observed in the mice receiving combinations with amiloride (Supplementary Fig. S8C).

Amiloride induces gene and transcript isoforms expression changes

To determine the molecular basis of the anti-myeloma activity of amiloride, we performed RNA-Seq analysis in KMS12-BM and JJN3 cell lines, the most and the least sensitive, respectively, at the beginning of apoptosis (15%–25% cell death, assessed by CellTiter-Glo luminescent assays) after amiloride treatment. The study design is shown in Supplementary Fig. S9. RNA-Seq data were analyzed at three levels: gene, isoform and splicing events. Although there were clearly more deregulated genes in KMS12-BM (almost 5,000) than in the JJN3 cell line (almost 1,000; Fig. 4A), significant enrichment of functional categories, such as metabolic, MAPK, and Jak–STAT signaling pathways, and endocytosis (Supplementary Fig. S10A), were found among the genes deregulated in both cell lines after amiloride treatment. The analysis of differential expression at the isoform level identified a similar number of deregulated transcript isoforms (over 15,000) in both cell lines (Supplementary Fig. S10B).

Next, we focused our analysis on those genes with a total expression that was not differentially modified after amiloride treatment, but whose transcript isoforms were differentially expressed. We found a considerable number of genes that were significantly deregulated at the isoform but not the gene level in both cell lines (Fig. 4B). Among the most significantly enriched pathways with deregulated transcript isoforms, in both cell lines, were those of the spliceosome, apoptosis, metabolic pathways, and those associated with protein-processing in ER, oxidative phosphorylation, cell cycle, RNA transport, and endocytosis (Fig. 4C). Transcript isoforms belonging to different components of the spliceosome and that are involved in the assembly and regulation of the spliceosomal machinery were significantly deregulated after amiloride treatment (Supplementary Table S3). For example, the transcript ENST00000269601, which encodes the canonical protein TXNL4A, is upregulated in myeloma cells treated with amiloride, whereas the transcript ENST00000588162, which encodes a smaller protein, was only expressed in untreated cells. Notably, the p53 pathway was only highly enriched in p53-expressing cell line, KMS12-BM, but not in the p53-null cell line, JJN3 (Fig. 4C; Supplementary Table S4).

Finally, using Multivariate Analysis of Transcript Splicing software we identified thousands of alternative splicing (AS) events in both cell lines after amiloride exposure (Fig. 4D). Most of the significant AS events (FDR < 0.05) involved genes whose total

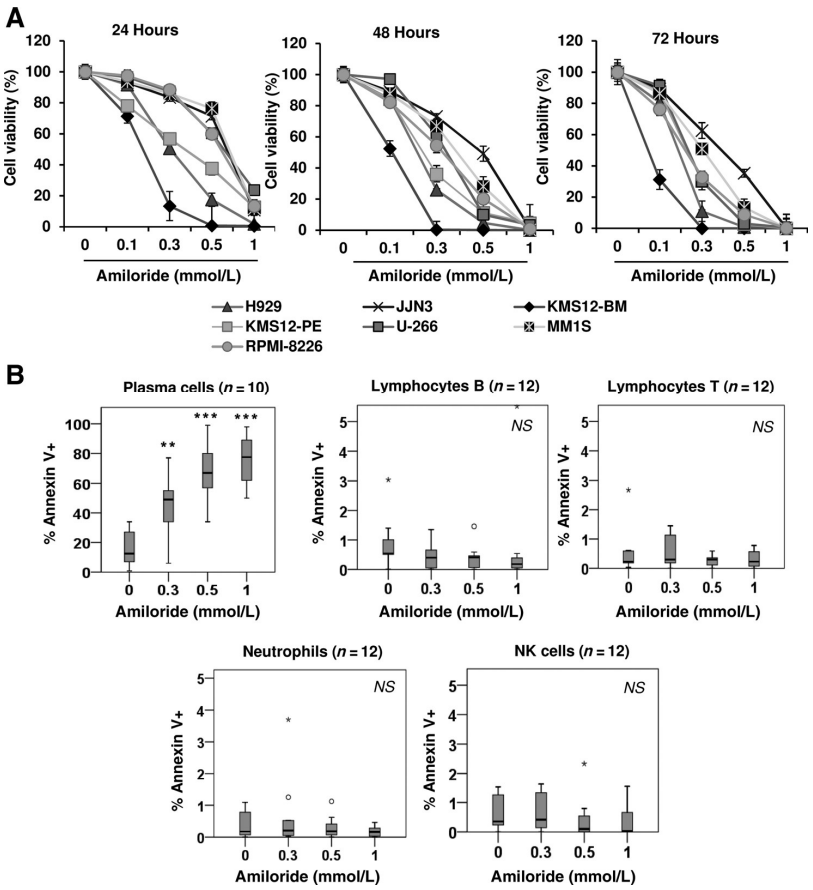

Figure 1.

Antimyeloma activity of amiloride in *in vitro* and *ex vivo* studies. **A,** The indicated multiple myeloma cell lines were incubated with increasing concentrations of amiloride for 24, 48, and 72 hours. Cell viability was analyzed by CellTiter-Glo luminescent assays. The average luminescent values of the untreated control samples were taken as 100%. Results are the means of three independent experiments. The statistically significant differences between untreated and treated cell lines were determined with Student *t* test. **B,** Bone marrow cells from patients with multiple myeloma, were treated *ex vivo* with increasing concentrations of amiloride for 48 hours. After the incubation period, cells were stained with the combination of Annexin V-FITC and three mAbs (CD45-PerCP-Cy5.5, CD38-APC and CD56 or CD19-PE) for the analysis of apoptosis in plasma cells. A panel of five antibodies in combination with Annexin V was used for the analysis of apoptosis in T and B lymphocytes, NK cells, and granulocytes. Results are presented as the percentage of Annexin V-positive cells. Statistically significant differences are represented as ***, FDR < 0.001 and **, FDR < 0.01 (Mann–Whitney *U* test). (*Continued on the following page.*)

expression was not modified by amiloride, indicating that the deregulation of alternative splicing could be a specific mechanism of action of amiloride. The most common AS event in both cell lines was the SE, which is the most common splice event in mammalian pre-mRNAs.

Amiloride modulates alternative splicing machinery

Given that RNA-Seq results showed deregulation of alternative splicing and spliceosome components in myeloma cells, we next evaluated whether the antimyeloma effect of amiloride was associated with modulation of the splicing machinery. The immunofluorescent staining for the SR (serine/arginine-rich) protein SC35 demonstrated the amiloride-induced modulation of the splicing machinery in myeloma cells with distinct *TP53* status. Thus, the modulation of the splicing machinery was accompanied by a reduction in cell viability in the H929 and JJN3 cell lines (Fig. 5). In both settings, the number of speckles was reduced but the remaining speckles increased in size and intensity. This finding was confirmed *in vivo* (Supplementary Fig. S11A) using xenografts inoculated with other multiple myeloma cell lines. Structural changes of the nuclear speckles induced by amiloride were also observed in $CD138^+$ cells from one newly diagnosed multiple myeloma patient (Supplementary Fig. S11B). In addition, mRNA levels of the spliceosome

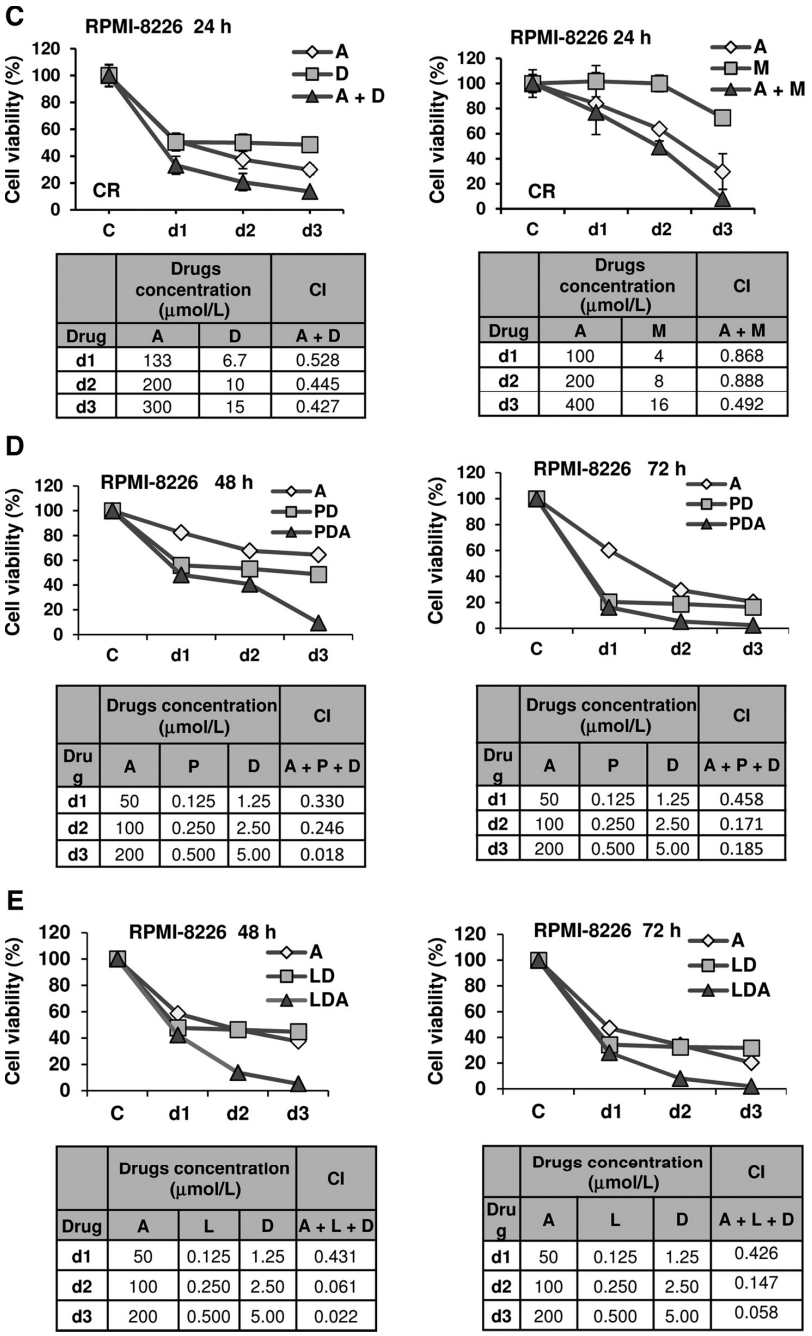

	Drugs concentration (μmol/L)		CI
Drug	A	D	A + D
d1	133	6.7	0.528
d2	200	10	0.445
d3	300	15	0.427

	Drugs concentration (μmol/L)		CI
Drug	A	M	A + M
d1	100	4	0.868
d2	200	8	0.888
d3	400	16	0.492

	Drugs concentration (μmol/L)			CI
Drug	A	P	D	A + P + D
d1	50	0.125	1.25	0.330
d2	100	0.250	2.50	0.246
d3	200	0.500	5.00	0.018

	Drugs concentration (μmol/L)			CI
Drug	A	P	D	A + P + D
d1	50	0.125	1.25	0.458
d2	100	0.250	2.50	0.171
d3	200	0.500	5.00	0.185

	Drugs concentration (μmol/L)			CI
Drug	A	L	D	A + L + D
d1	50	0.125	1.25	0.431
d2	100	0.250	2.50	0.061
d3	200	0.500	5.00	0.022

	Drugs concentration (μmol/L)			CI
Drug	A	L	D	A + L + D
d1	50	0.125	1.25	0.426
d2	100	0.250	2.50	0.147
d3	200	0.500	5.00	0.058

Figure 1.

(*Continued.*) RPMI-8226 cell line was treated with the indicated double combinations of amiloride with melphalan or dexamethasone (**C**) and triple combinations with pomalidomide or lenalidomide plus dexamethasone (**D**, **E**). Cell viability was assessed by MTT assay, as represented in the graphs. The combination indexes (CI) were calculated with the CalcuSyn software. CIs of <0.3, 0.3–0.7, 0.7–0.85, 0.85–0.90, 0.90–1.10, and >1.10 indicate strong synergism, synergism, moderate synergism, slight synergism, additive effect, and antagonism, respectively. C, control; A, amiloride; D, dexamethasone; M, melphalan; P, pomalidomide; L, lenalidomide; d1, d2, and d3, drug concentrations used in the study; CR, constant ratio.

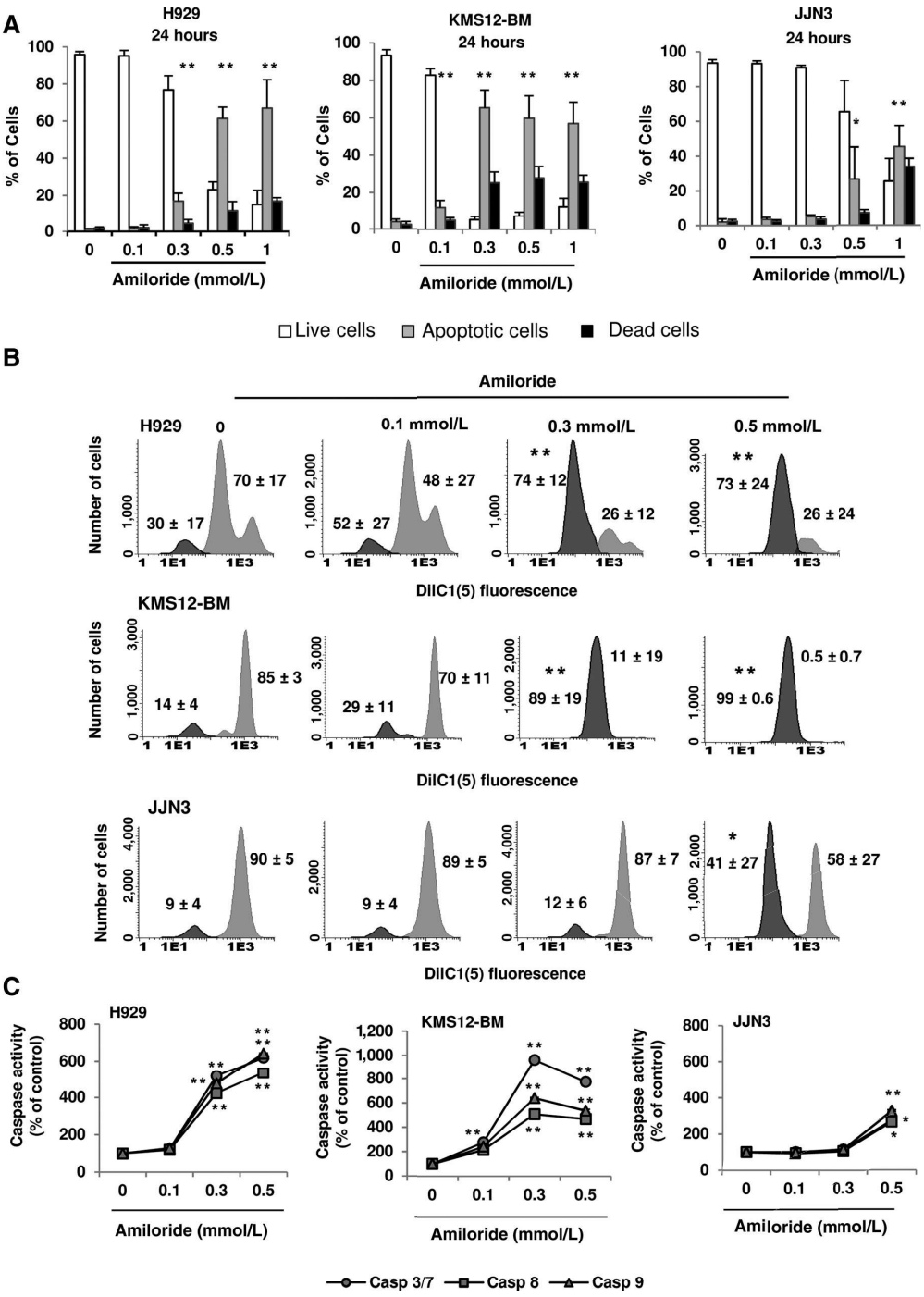

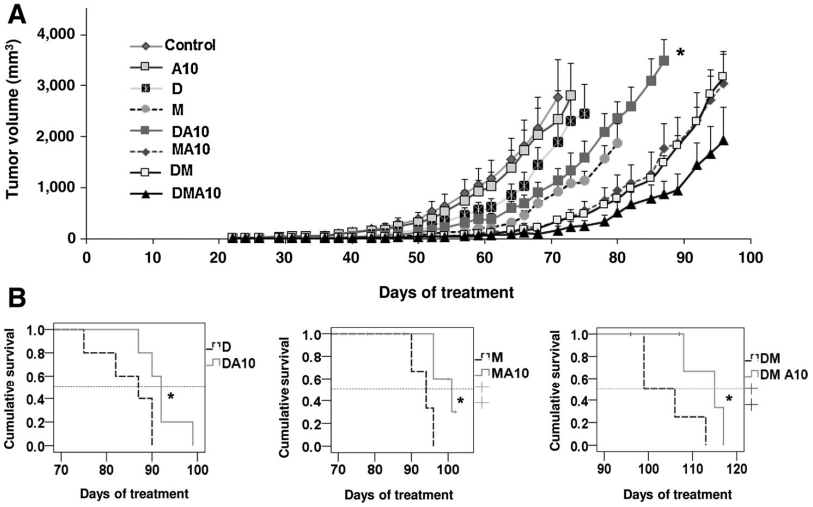

Figure 3.

The triple and double combination of dexamethasone and melphalan with amiloride displays superior anti-multiple myeloma activity and improves median survival compared with single agents and double combinations in a subcutaneous plasmacytoma model. CB17-SCID mice subcutaneously inoculated with 3×10^6 MM1S cells in the right flank were randomized to receive vehicle, amiloride (10 mg/kg, oral, daily), dexamethasone (0.5 mg/kg, i.p., 2 days per week), melphalan (2.5 mg/kg, i.p., 2 days per week) in monotherapy and the respective double and triple combinations ($n = 5$/group). **A,** Evolution of tumor volumes of the plasmacytomas. Statistical differences between groups were evaluated fitting an exponential regression model and the regression parameters were compared using a *t* test for unequal variances. Bars indicate SEM. **B,** Kaplan–Meier curves representing the survival of each treatment group. Mice were sacrificed when their tumor diameters reached 2 cm or when they became moribund. Statistically significant differences were analyzed by the log-rank test, and are represented as *, $P < 0.05$.

components (SNRNP27, SRSF4, SF3B1, LSM3, LSM14A, PRPF3, and PRPF4) were significantly overexpressed in myeloma cells from patients after amiloride treatment (Supplementary Fig. S11C). Altogether, these results suggest the potential association between the antimyeloma activity of amiloride and the modulation of spliceosomal machinery.

Antimyeloma activity of amiloride is associated with functional p53 signaling

Our results showed that multiple myeloma cells either with WT or mutated *TP53* were highly sensitive to amiloride, although higher doses and longer exposure to amiloride were required for p53-null cells. Moreover, pathway enrichment analysis from RNA-Seq data in mutated *TP53* cells revealed a subset of deregulated transcript isoforms involved in the p53 pathway. These findings suggest an activation of p53 signaling pathway in multiple myeloma cells after treatment with amiloride. To test this hypothesis, we used qRT-PCR to measure the expression of p53 targets, such as *BAK1*, *BBC3*, *TNFRSF10B*, *FAS*, *CDKN1B*, and *CDKN1A* in multiple myeloma cell lines with different *TP53* status. We observed a normal functional p53 response in the WT/WT cell line (MM1S), whereas p53 signaling was abrogated in JJN3 cells with no basal p53 expression (Fig. 6A). Interestingly, the mutated *TP53* cell lines (KMS12-BM and U-266) also showed overexpression of p53 targets. Similar results were found by RNA-Seq data analysis (Supplementary Fig. S12). The activation of p53 signaling pathway was confirmed in $CD138^+$ cells from eight multiple myeloma patients after treatment with amiloride (Supplementary Fig. S13)

The cell lines with mutated *TP53* showed deregulation of p53 targets after treatment with amiloride, so we decided to confirm the involvement of p53 in amiloride-induced cytotoxicity of multiple myeloma cells. The functionality of p53 signaling pathway in mutated *TP53* cell lines was confirmed using p53 activity inhibitors: pifithrin-α (PFTα), a reversible inhibitor of p53-mediated apoptosis and p53-dependent gene transcription (21), and pifithrin-μ (PFTμ), an inhibitor of the p53–Bcl-xL interaction that directly inhibits p53 binding to mitochondria (22). Amiloride cytotoxicity was reduced in WT and mutated *TP53* multiple myeloma cell lines when used with p53 inhibitors. As expected, the inhibitors had no effect on the death of JJN3 cells, which lack p53 expression (Fig. 6B). These results imply that p53 signaling

Figure 2.

Amiloride induces apoptosis, activates caspases, and deregulates mitochondrial potential in multiple myeloma cell lines. H929, JJN3, and KMS12-BM cells were treated with increasing concentrations of amiloride for 24 hours. **A,** The induction of apoptosis was analyzed by flow cytometry after Annexin-V/PI staining. **B,** Mitochondrial membrane depolarization was examined by flow cytometry after DiIC1(5) staining. **C,** The activity of caspase-8, caspase-9, and caspase-3/7 was analyzed by luminescent caspase assays. Results are expressed as the mean ± SD of three independent experiments. Statistically significant differences between untreated and treated cell lines are represented as **, $P < 0.01$ and *, $P < 0.05$ (Student *t* test).

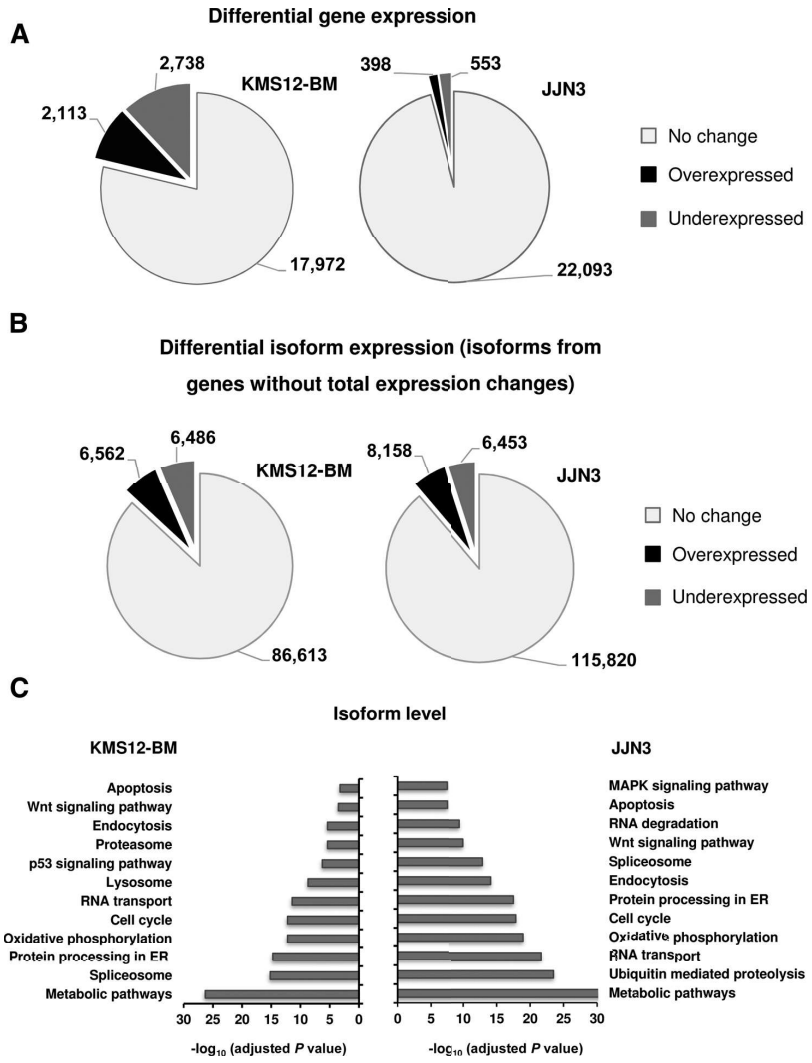

Figure 4.
Amiloride induces gene and isoform expression changes and modulates alternative splicing. RNA sequencing analysis was conducted on Poly A+ RNA from KMS12-BM and JJN3 cell lines, treated, or untreated with amiloride (0.1 mmol/L and 0.4 mmol/L, respectively) for 24 hours. **A,** Distribution of differentially expressed genes induced by amiloride (overexpressed with FC $\geq$ 2 and FDR < 0.05; underexpressed with FC $\leq$ -2 and FDR < 0.05 and not deregulated genes), identified using the DESeq2 R package. **B,** Distribution of differentially expressed transcript isoforms contained in genes without expression changes, identified using Cuffdiff. Only the isoforms that have a |FC|$\geq$ 2 were considered as differentially expressed. **C,** Summary of the biologically relevant pathways among the top 50 significantly enriched pathways in KEGG enrichment analysis for amiloride-deregulated isoforms detected in KMS12-BM (left) and JJN3 (right) cell lines. Statistical significance of the enrichment is expressed as -log10 (Benjamini–Hochberg adjusted *P* value). (*Continued on the following page.*)

has an important role in amiloride-induced apoptosis of multiple myeloma cells that express either WT or mutated *TP53*. On the other hand, the involvement of a mechanism other than p53 signaling activation would explain the antimyeloma effect of amiloride on p53-null cells.

Discussion

In this study, we demonstrate for the first time the antimyeloma activity of amiloride, an antihypertensive drug, through two novel mechanisms of action, spliceosome deregulation and p53 signaling pathway activation. Initially, we observed potent *in vitro* antimyeloma activity of amiloride, both in *TP53* wild-type and mutated *TP53* cells. Even in p53-null cells, viability was reduced by using higher doses and longer exposures. The *ex vivo* study of myeloma cells from patients indicated that amiloride induced cytotoxicity in plasma cells, including three cases bearing deletion of 17p, whereas viability of other bone marrow cell populations was not affected. Furthermore, amiloride in combination with dexamethasone and melphalan was clearly synergic *in vitro*. A synergic effect was also observed when amiloride was combined with lenalidomide or pomalidomide plus dexamethasone. In this context, amiloride has been described as potentiating synergistically the antiproliferative effect of other drugs like imatinib, the first-line therapy for patients with chronic myeloid leukemia (CML; refs. 23, 24). However, we did not find synergism between amiloride and bortezomib, which could limit the use of amiloride in bortezomib-based induction regimens.

The induction of apoptosis by amiloride in CML was accompanied by the increase in levels of caspases 9 and 3. Our results

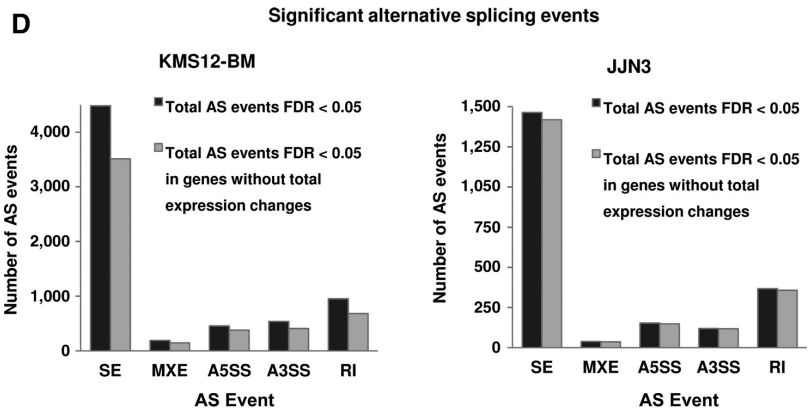

	SE	MXE	A5SS	A3SS	RI		SE	MXE	A5SS	A3SS	RI
KMS12-BM	4484	192	458	539	953	Total AS events FDR < 0.05	1465	39	154	120	369
KMS12-BM	3512 (78%)	145 (76%)	379 (83%)	408 (76%)	684 (72%)	Total AS events FDR < 0.05 in genes without total expression changes	1419 (97%)	37 (95%)	148 (96%)	118 (98%)	358 (97%)

Figure 4.
(*Continued.*) **D,** Alternative splicing events in genes without expression changes were detected using rMATS and classified into five main types of pattern: skipped exon (SE), mutually exclusive exons (MXE), alternative 5′ splice site (A5SS), alternative 3′ splice site (A3SS), and retained introns (RI). rMATS also calculates the difference in the ratio of these events between two conditions, producing a false discovery rate.

showed that the apoptosis induced by amiloride was mediated by both caspase-dependent and caspase-independent mechanisms, which is consistent with other studies in glioblastoma and breast tumor cells (25–27). Moreover, we observed increased survival of mice bearing human subcutaneous plasmacytomas treated with double or triple combinations including amiloride compared with treatment with melphalan and/or dexamethasone.

The anticancer effect of amiloride has previously been described in several tumors, using *in vitro* and *in vivo* models (9, 23–33). There is evidence for multiple mechanisms of action of amiloride, including TRAIL-induced cytotoxicity associated with the PI3K-Akt pathway (24, 28, 30, 33) and alternative splicing deregulation of apoptotic genes (9, 23, 28). The RNA-Seq allowed us to study its mechanism of action in myeloma cells more extensively. In fact, RNA-Seq analysis in two cell lines with distinct patterns of response to the drug, the most and the least sensitive, revealed that amiloride significantly altered the level of transcript isoforms and the alternative splicing events. It should be pointed out that the significant impact on the differential expression of isoforms from genes whose total expression was not changed. In other words, the traditional gene expression profiling would have overlooked the substantial modifications of more than 10,000 transcript isoforms by amiloride treatment. These results are consistent with the reported advantage of the analysis at the genome-wide isoform level compared with gene expression in cancer research (34, 35).

One of the most significantly enriched pathways in the analysis of differentially expressed isoforms after amiloride treatment was spliceosome. We found that amiloride induced a general deregulation of spliceosomal machinery at the gene and transcript isoform levels that affected the early and late stages of spliceosome assembly and several spliceosome-associated proteins, including the catalytic steps of the splicing. These findings, together with the large quantity of total transcript isoforms modified by amiloride, prompted us to investigate further the influence of amiloride in the pre-mRNA splicing machinery. The small nuclear ribonucleoproteins (snRNP) and splicing factors, like the SR protein family, are organized in nuclear speckles (36). The changes in protein SC35-staining speckles are used as a marker for the disruption of the splicing machinery (37–40). Upon the inhibition of the splicing machinery, the number of nuclear speckles decreases but those remaining increase in size and intensity (36, 41). Using this marker, after amiloride treatment, we identified a similar pattern of nuclear speckle modifications that was associated with cell viability inhibition. This finding indicates that amiloride provokes the disruption of the splicing machinery and that this could, in turn, induce cytotoxicity.

The RNA-Seq analysis at the transcript isoform level also identified the p53 pathway as one of the most significantly enriched functional categories. Remarkably, the p53 pathway was highly overexpressed only in the cell line expressing mutated *TP53*, and not in the p53-null cell line. In addition, upregulation of p53 targets was observed in WT and mutated *TP53* myeloma cells treated with amiloride. These results, together with the fact that the inhibition of p53 protein activity prevents amiloride-induced cell death, even in two mutated *TP53* cell lines, demonstrate that amiloride-induced apoptosis in myeloma cells is dependent on p53 activation and is independent of the mutational status of *TP53*. Apart from that, the reduction in cell viability in the amiloride-treated p53-null cell line supports the notion that other mechanisms independent of p53, such as the

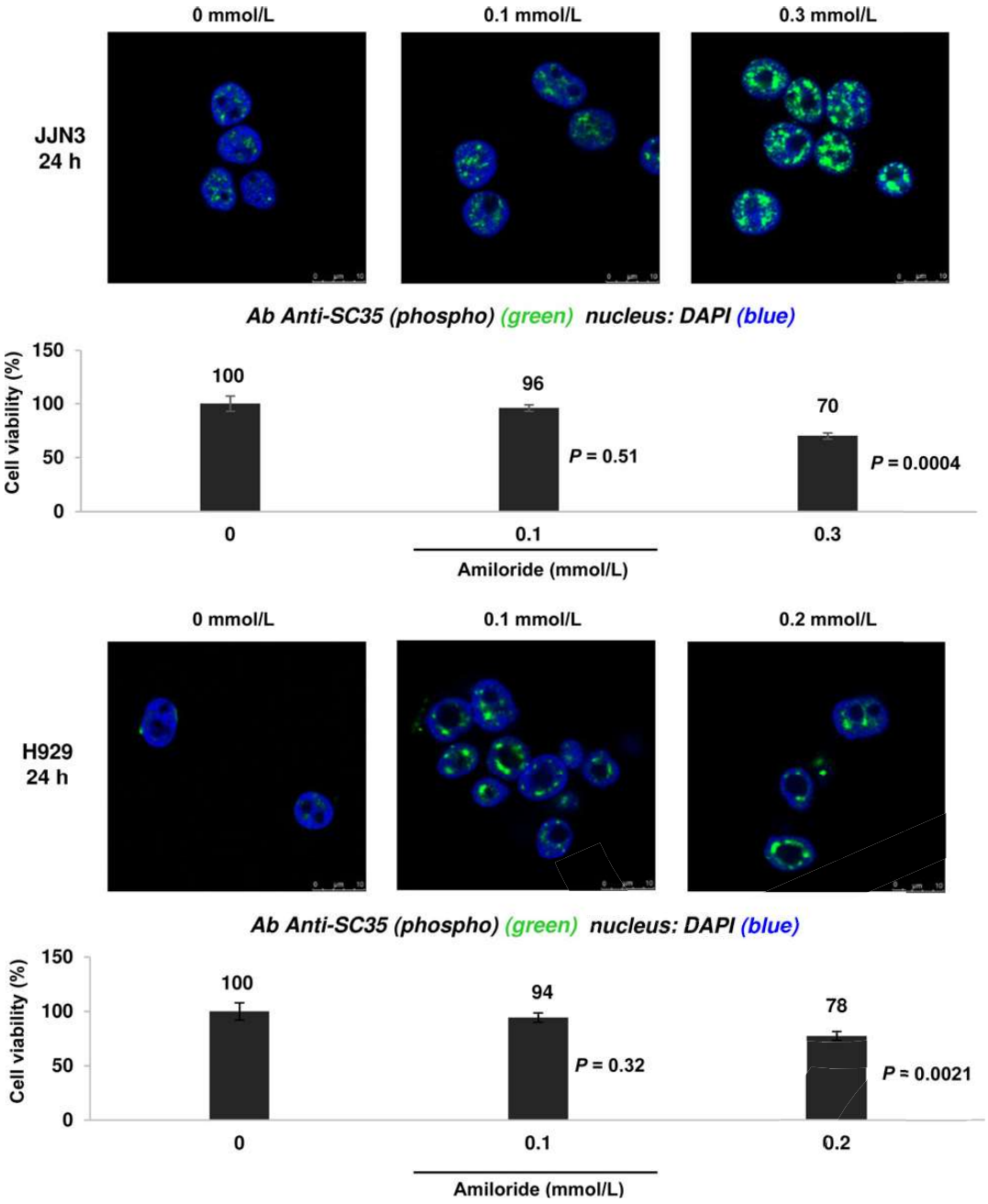

Figure 5.
Amiloride affects the pre-mRNA splicing machinery in myeloma cells *in vitro*, independently of *TP53* status. H929 (*TP53* WT) and JJN3 (*TP53* null) cells were treated with increasing concentrations of amiloride. SC35-staining nuclear speckles were detected by immunofluorescence after 24 hours. Cell viability was analyzed by CellTiter-Glo luminescent assays and expressed as the mean ± SD. Statistically significant differences between amiloride-treated and untreated cells are presented. *P* values were assessed by the two-sided Student *t* test.

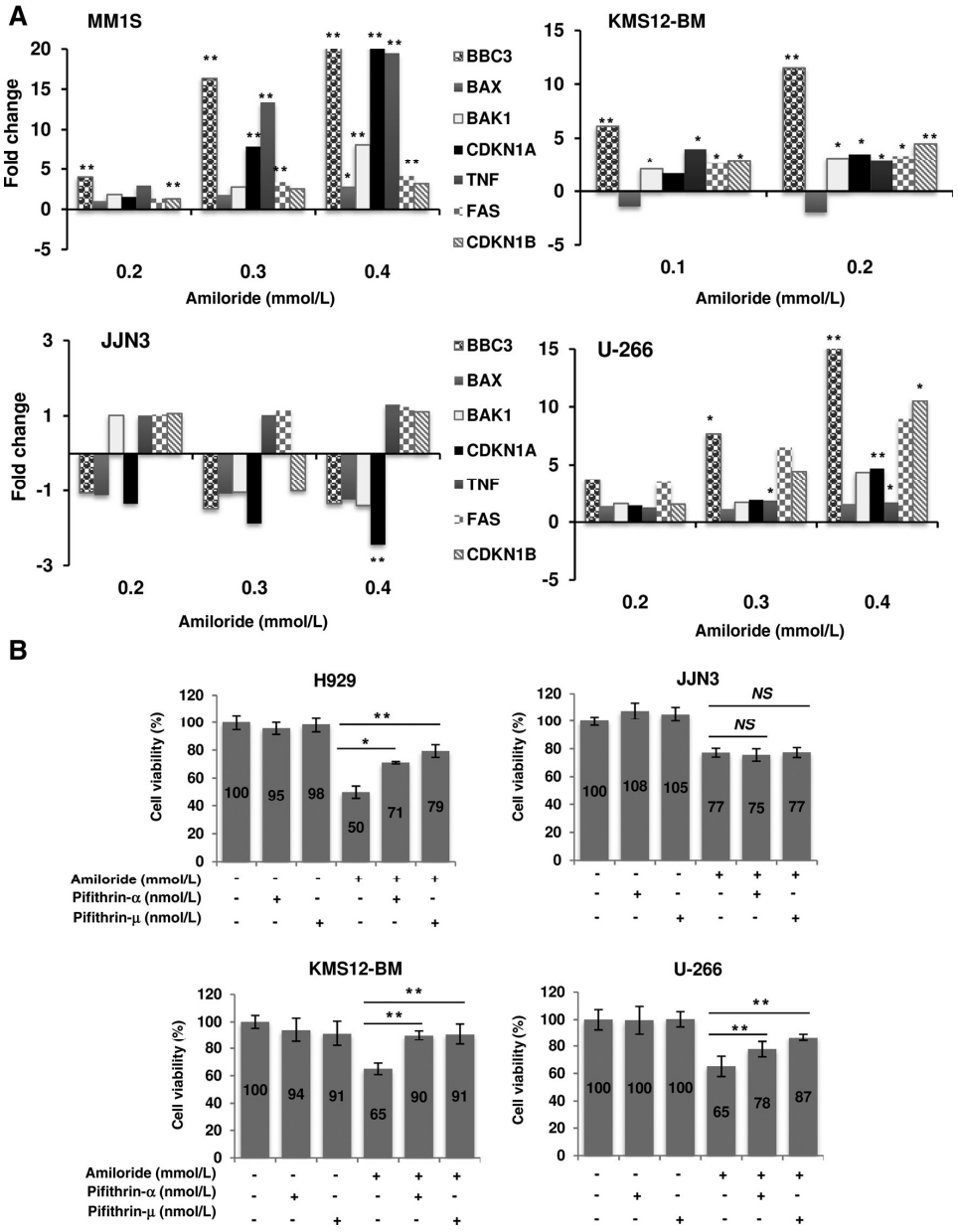

Figure 6.

The p53 signaling pathway is activated in *TP53* WT and MUT, but not in p53-null multiple myeloma cells. **A,** MM1S, KMS12-BM, JJN3, and U-266 cells were treated with increasing concentrations of amiloride. mRNA levels of *BBC3* (*PUMA*), *BAX, BAK1, CDKN1A* (*p21*), *CDKN1B, TNFRSF10B*, and *FAS* (*CD95*), were assessed by qRT-PCR 24 hours after amiloride treatment. The results are shown as the magnitude of change between treated and untreated cells and correspond to the average of three experiments after normalization with 18S rRNA. Statistically significant differences between untreated and treated cell lines are represented as **, $P < 0.01$ and *, $P < 0.05$ (Student *t* test). **B,** Cell viability upon amiloride (KMS12-BM at 0.1 mmol/L; H929 at 0.2 mmol/L; JJN3 and U-266 at 0.3 mmol/L), pifithrin-α (10 nmol/L) or pifithrin-μ (2.5 nmol/L) treatment was analyzed by CellTiter-Glo luminescent assays, 24 hours after amiloride treatment. Results are the mean of at least three independent experiments. Asterisks indicate statistically significant differences between amiloride-treated cells and amiloride-pifithrin-α/μ-treated cells; **, $P < 0.01$; *, $P < 0.05$; *N.S.*, no significant (Student *t* test).

spliceosomal machinery disruption observed in JJN3 cell line, are involved in amiloride activity.

Amiloride has been used for many years as adjuvant treatment with thiazide diuretics in congestive heart failure and hypertension (42–45). Here, we demonstrate for the first time the therapeutic potential of amiloride in multiple myeloma. The concentration of amiloride used in the *in vivo* experiments is higher than that commonly used as a potassium-sparing diuretic, suggesting that a higher dose would be needed to produce the anti-multiple myeloma effect. The toxicity profile of this drug is very well known and the main side effect is hyperkalemia, which could be the main factor that limits the use of amiloride as an antimyeloma drug. To minimize this risk, a careful electrolyte monitoring along with the coadministration of a kaliuretic agent or the use of new oral agents for the hyperkalemia treatment, such as patiromer calcium (46–48) and ZS-9 (zirconium cyclosilicate; refs. 48–50), could be required. Moreover, attempts to develop amiloride analogues that show reduced diuretic and antikaliuretic effects retaining or enhancing anticancer activity are currently underway in different laboratories. On the other hand, as reported in other studies (23, 32), we did not find any significant systemic toxicity in the mice treated with amiloride, and the viability of the lymphocyte population either from multiple myeloma patients or healthy donors was not affected, even at the highest dose.

Our results also revealed that the antimyeloma activity of amiloride was mediated through spliceosome modulation and involved the p53 pathway. In fact, p53 signaling was activated after amiloride exposure, independently of the mutational status of *TP53*. On the other hand, amiloride was also able to induce apoptosis in myeloma cells that did not express p53.

In conclusion, these findings together with the possibility of combining amiloride with melphalan, dexamethasone, or lenalidomide or pomalidomide, support the initiation of clinical trials including amiloride for patients with relapsed and refractory multiple myeloma, particularly for those with 17p deletion or *TP53* mutations who display a poor prognosis.

Disclosure of Potential Conflicts of Interest

No potential conflicts of interest were disclosed.

Authors' Contributions

Conception and design: E.A. Rojas, I. Misiewicz-Krzeminska, N.C. Gutiérrez
Development of methodology: E.A. Rojas, J.F. Martínez-Blanch, I. Misiewicz-Krzeminska
Acquisition of data (provided animals, acquired and managed patients, provided facilities, etc.): E.A. Rojas, L. San-Segundo, J.F. Martínez-Blanch, F.M. Codoñer, T. Paíno, N. Puig, M. Victoria Mateos, N.C. Gutiérrez
Analysis and interpretation of data (e.g., statistical analysis, biostatistics, computational analysis): E.A. Rojas, L.A. Corchete, J.F. Martínez-Blanch, F.M. Codoñer, T. Paíno, N. Puig, E.M. Ocio, N.C. Gutiérrez
Writing, review, and/or revision of the manuscript: E.A. Rojas, L.A. Corchete, F.M. Codoñer, N. Puig, R. García-Sanz, M. Victoria Mateos, E.M. Ocio, I. Misiewicz-Krzeminska, N.C. Gutiérrez
Administrative, technical, or material support (i.e., reporting or organizing data, constructing databases): N. Puig, R. García-Sanz, N.C. Gutiérrez
Study supervision: R. García-Sanz, I. Misiewicz-Krzeminska, N.C. Gutiérrez

Acknowledgments

The authors thank Isabel Isidro, Teresa Prieto, Vanesa Gutiérrez, Irene Aires, and José Pérez for their technical assistance; Lorena González for the help with the assays of the combinations of antimyeloma drugs; Mercedes Garayoa for the help with MSC studies; and Phil Mason for his help in reviewing the English language of the manuscript.

Grant Support

This study was partially supported by the Instituto de Salud Carlos III-Cofinanciación with funding from FEDER (PI13/00111 and PI16/01074), Asociación Española Contra el Cáncer (AECC, GCB120981SAN), Gerencia Regional de Salud, Junta de Castilla y León (BIO/SA57/13 and BIO/SA22/15), and the INNOCAMPUS Program (CEI10-1-0010). I. Misiewicz-Krzeminska was supported by a Black Swan Research Initiative® grant from the International Myeloma Foundation. L.A. Corchete was supported by a grant from the Fundación Española de Hematología y Hemoterapia.

The costs of publication of this article were defrayed in part by the payment of page charges. This article must therefore be hereby marked *advertisement* in accordance with 18 U.S.C. Section 1734 solely to indicate this fact.

Received March 8, 2017; revised June 30, 2017; accepted July 28, 2017; published OnlineFirst August 8, 2017.

References

1. Kumar SK, Rajkumar SV, Dispenzieri A, Lacy MQ, Hayman SR, Buadi FK, et al. Improved survival in multiple myeloma and the impact of novel therapies. Blood 2008;111:2516–20.
2. Kumar SK, Dispenzieri A, Lacy MQ, Gertz MA, Buadi FK, Pandey S, et al. Continued improvement in survival in multiple myeloma: changes in early mortality and outcomes in older patients. Leukemia 2014;28:1122–8.
3. Mateos M-V, Ocio EM, Paiva B, Rosiñol L, Martínez-López J, Bladé J, et al. Treatment for patients with newly diagnosed multiple myeloma in 2015. Blood Rev 2015;29:387–403.
4. Kumar SK, Lee JH, Lahuerta JJ, Morgan G, Richardson PG, Crowley J, et al. Risk of progression and survival in multiple myeloma relapsing after therapy with IMiDs and bortezomib: a multicenter international myeloma working group study. Leukemia 2012;26:149–57.
5. Rajan AM, Kumar S. New investigational drugs with single-agent activity in multiple myeloma. Blood Cancer J 2016;6:e451.
6. Würth R, Thellung S, Bajetto A, Mazzanti M, Florio T, Barbieri F. Drug-repositioning opportunities for cancer therapy: novel molecular targets for known compounds. Drug Discov Today 2016;21:190–9.
7. Tang CM, Presser F, Morad M. Amiloride selectively blocks the low threshold (T) calcium channel. Science 1988;240:213–5.
8. Slepkov ER, Rainey JK, Sykes BD, Fliegel L. Structural and functional analysis of the Na+/H+ exchanger. Biochem J 2007;401:623–33.
9. Chang J-G, Yang D-M, Chang W-H, Chow L-P, Chan W-L, Lin H-H, et al. Small molecule amiloride modulates oncogenic RNA alternative splicing to devitalize human cancer cells. PLoS One 2011;6:e18643.
10. Tazi J, Bakkour N, Stamm S. Alternative splicing and disease. Biochim Biophys Acta 2009;1792:14–26.
11. Wang G-S, Cooper TA. Splicing in disease: disruption of the splicing code and the decoding machinery. Nat Rev Genet 2007;8:749–61.
12. Cartegni L, Chew SL, Krainer AR. Listening to silence and understanding nonsense: exonic mutations that affect splicing. Nat Rev Genet 2002;3:285–98.
13. Venables JP. Aberrant and alternative splicing in cancer. Cancer Res 2004;64:7647–54.
14. Kim E, Goren A, Ast G. Insights into the connection between cancer and alternative splicing. Trends Genet 2008;24:7–10.
15. Misiewicz-Krzeminska I, Sarasquete ME, Quwaider D, Krzeminski P, Ticona FV, Paíno T, et al. Restoration of microRNA-214 expression reduces growth of myeloma cells through positive regulation of P53 and inhibition of DNA replication. Haematologica 2013;98:640–8.
16. Maiso P, Carvajal-Vergara X, Ocio EM, López-Pérez R, Mateo G, Gutiérrez N, et al. The histone deacetylase inhibitor LBH589 is a potent antimyeloma agent that overcomes drug resistance. Cancer Res 2006;66:5781–9.

17. Chou T-C. Drug combination studies and their synergy quantification using the Chou-Talalay method. Cancer Res 2010;70:440–6.
18. Ocio EM, Vilanova D, Atadja P, Maiso P, Crusoe E, Fernández-Lázaro D, et al. In vitro and in vivo rationale for the triple combination of panobinostat (LBH589) and dexamethasone with either bortezomib or lenalidomide in multiple myeloma. Haematologica 2010;95:794–803.
19. Shen S, Park JW, Lu Z, Lin L, Henry MD, Wu YN, et al. rMATS: robust and flexible detection of differential alternative splicing from replicate RNA-Seq data. Proc Natl Acad Sci U S A 2014;111:E5593–5601.
20. Wang J, Duncan D, Shi Z, Zhang B. WEB-based GEne SeT AnaLysis Toolkit (WebGestalt): update 2013. Nucleic Acids Res 2013;41:W77–83.
21. Farah IO, Begum RA, Ishaque AB. Differential protection and transactivation of P53, P21, Bcl2, PCNA, cyclin G, and MDM2 genes in rat liver and the HepG2 cell line upon exposure to pifithrin. Biomed Sci Instrum 2007;43:116–21.
22. Hagn F, Klein C, Demmer O, Marchenko N, Vaseva A, Moll UM, et al. BclxL changes conformation upon binding to wild-type but not mutant p53 DNA binding domain. J Biol Chem 2010;285:3439–50.
23. Chang W-H, Liu T-C, Yang W-K, Lee C-C, Lin Y-H, Chen T-Y, et al. Amiloride modulates alternative splicing in leukemic cells and resensitizes Bcr-AblT315I mutant cells to imatinib. Cancer Res 2011;71:383–92.
24. Zheng Y, Yang H, Li T, Zhao B, Shao T, Xiang X, et al. Amiloride sensitizes human pancreatic cancer cells to erlotinib in vitro through inhibition of the PI3K/AKT signaling pathway. Acta Pharmacol Sin 2015;36:614–26.
25. Leon LJ, Pasupuleti N, Gorin F, Carraway KL. A cell-permeant amiloride derivative induces caspase-independent, AIF-mediated programmed necrotic death of breast cancer cells. PLoS One 2013;8:e63038.
26. Hegde M, Roscoe J, Cala P, Gorin F. Amiloride kills malignant glioma cells independent of its inhibition of the sodium-hydrogen exchanger. J Pharmacol Exp Ther 2004;310:67–74.
27. Harley W, Floyd C, Dunn T, Zhang X-D, Chen T-Y, Hegde M, et al. Dual inhibition of sodium-mediated proton and calcium efflux triggers non-apoptotic cell death in malignant gliomas. Brain Res 2010;1363:159–69.
28. Tang J-Y, Chang H-W, Chang J-G. Modulating roles of amiloride in irradiation-induced antiproliferative effects in glioblastoma multiforme cells involving Akt phosphorylation and the alternative splicing of apoptotic genes. DNA Cell Biol 2013;32:504–10.
29. Yang X, Wang D, Dong W, Song Z, Dou K. Suppression of Na+/H + exchanger 1 by RNA interference or amiloride inhibits human hepatoma cell line SMMC-7721 cell invasion. Med Oncol Northwood 2011;28:385–90.
30. Cho Y-L, Lee K-S, Lee S-J, Namkoong S, Kim Y-M, Lee H, et al. Amiloride potentiates TRAIL-induced tumor cell apoptosis by intracellular acidification-dependent Akt inactivation. Biochem Biophys Res Commun 2005; 326:752–8.
31. Sparks RL, Pool TB, Smith NK, Cameron IL. Effects of amiloride on tumor growth and intracellular element content of tumor cells in vivo. Cancer Res 1983;43:73–7.
32. Matthews H, Ranson M, Kelso MJ. Anti-tumour/metastasis effects of the potassium-sparing diuretic amiloride: an orally active anti-cancer drug waiting for its call-of-duty? Int J Cancer 2011;129:2051–61.
33. Kim KM, Lee YJ. Amiloride augments TRAIL-induced apoptotic death by inhibiting phosphorylation of kinases and phosphatases associated with the P13K-Akt pathway. Oncogene 2005;24:355–66.
34. Zhang C, Li H-R, Fan J-B, Wang-Rodriguez J, Downs T, Fu X-D, et al. Profiling alternatively spliced mRNA isoforms for prostate cancer classification. BMC Bioinformatics 2006;7:202.
35. Zhang Z, Pal S, Bi Y, Tchou J, Davuluri RV. Isoform level expression profiles provide better cancer signatures than gene level expression profiles. Genome Med 2013;5:33.
36. Shepard PJ, Hertel KJ. The SR protein family. Genome Biol 2009; 10:242.
37. Kotake Y, Sagane K, Owa T, Mimori-Kiyosue Y, Shimizu H, Uesugi M, et al. Splicing factor SF3b as a target of the antitumor natural product pladienolide. Nat Chem Biol 2007;3:570–5.
38. Kaida D, Motoyoshi H, Tashiro E, Nojima T, Hagiwara M, Ishigami K, et al. Spliceostatin A targets SF3b and inhibits both splicing and nuclear retention of pre-mRNA. Nat Chem Biol 2007;3:576–83.
39. Allende-Vega N, Dayal S, Agarwala U, Sparks A, Bourdon J-C, Saville MK. p53 is activated in response to disruption of the pre-mRNA splicing machinery. Oncogene 2013;32:1–14.
40. Ghosh G, Adams JA. Phosphorylation mechanism and structure of serine-arginine protein kinases. FEBS J 2011;278:587–97.
41. Spector DL, Lamond AI. Nuclear speckles. Cold Spring Harb Perspect Biol 2011;3:a000646.
42. Fuchs SC, Poli-de-Figueiredo CE, Figueiredo Neto JA, Scala LCN, Whelton PK, Mosele F, et al. Effectiveness of chlorthalidone plus amiloride for the prevention of hypertension: the PREVER-Prevention Randomized Clinical Trial. J Am Heart Assoc 2016;5:04248.
43. Andersen H, Hansen PBL, Bistrup C, Nielsen F, Henriksen JE, Jensen BL. Significant natriuretic and antihypertensive action of the epithelial sodium channel blocker amiloride in diabetic patients with and without nephropathy. J Hypertens 2016;34:1621–9.
44. Oxlund CS, Buhl KB, Jacobsen IA, Hansen MR, Gram J, Henriksen JE, et al. Amiloride lowers blood pressure and attenuates urine plasminogen activation in patients with treatment-resistant hypertension. J Am Soc Hypertens 2014;8:872–81.
45. Fuchs FD, Scala LCN, Vilela-Martin JF, de Mello RB, Mosele F, Whelton PK, et al. Effectiveness of chlorthalidone/amiloride versus losartan in patients with stage I hypertension: results from the PREVER-treatment randomized trial. J Hypertens 2016;34:798–806.
46. Weir MR, Bakris GL, Bushinsky DA, Mayo MR, Garza D, Stasiv Y, et al. Patiromer in patients with kidney disease and hyperkalemia receiving RAAS inhibitors. N Engl J Med 2015;372:211–21.
47. Bakris GL, Pitt B, Weir MR, Freeman MW, Mayo MR, Garza D, et al. Effect of patiromer on serum potassium level in patients with hyperkalemia and diabetic kidney disease: The AMETHYST-DN Randomized Clinical Trial. JAMA 2015;314:151–61.
48. Henneman A, Guirguis E, Grace Y, Patel D, Shah B. Emerging therapies for the management of chronic hyperkalemia in the ambulatory care setting. Am J Health Syst Pharm 2016;73:33–44.
49. Linder KE, Krawczynski MA, Laskey D. Sodium zirconium cyclosilicate (ZS-9): a novel agent for the treatment of hyperkalemia. Pharmacotherapy 2016;36:923–33.
50. Packham DK, Kosiborod M. Pharmacodynamics and pharmacokinetics of sodium zirconium cyclosilicate [ZS-9] in the treatment of hyperkalemia. Expert Opin Drug Metab Toxicol 2016;12:567–73.